SURFACE CHARACTERIZATION STUDY OF InP(100) SUBSTRATES

By

STUART JAMISON HOEKJE

A DISSERTATION PRESENTED TO THE GRADUATE SCHOOL
OF THE UNIVERSITY OF FLORIDA IN PARTIAL FULFILLMENT
OF THE REQUIREMENTS FOR THE DEGREE OF
DOCTOR OF PHILOSOPHY

UNIVERSITY OF FLORIDA

1990

UNIVERSITY OF FLORIDA LIBRARIES

... build a ladder to the stars,

and climb on every rung ...

R. Zimmerman

ACKNOWLEDGMENTS

The author wishes to thank his father and mother, James Wilbur and Cleora Ann Hoekje, for instilling in him the drive for wisdom and clarity. In particular he would like to thank his father, a caring and gentle teacher of scientific and engineering techniques. The author would also like to express his appreciation and gratitude to his wife, Lynn Marie Hoekje, for her support and patience, and her enduring love. She has returned the joy to his life. The author has been most fortunate to have had the timely assistance and guidance of Dr. Richard C. Alkire, chairman of the Chemical Engineering Department of the University of Illinois, Marcel J. Vogel, a retired senior chemist for IBM, and Alfred L. Arnold, a personal confidant. The author is sincerely grateful for the efforts made by his advisor, Dr. Gar B. Hoflund, a fine and generous man. The author has benefitted from the counsel of Dr. Mark E. Orazem, Dr. Gerry Lyberatos, and Dr. Lewis E. Johns, faculty members of the Chemical Engineering Department. He is grateful for their efforts. The author expresses his appreciation to the members of his committee, Dr. Herbert A. Laitinen and Dr. Vaneica Y. Young of the Chemistry Department and Dr. Dinesh O. Shah, department chairman of the Chemical Engineering Department. Lastly, the author wishes to thank Dr. Mark R. Davidson for his assistance.

TABLE OF CONTENTS

	page
ACKNOWLEDGMENTS	iii
ABSTRACT	v
INTRODUCTION	1
COMPARISON OF SUBSTRATE CLEANING TECHNIQUES	5
Introduction	5
Experimental	7
Results and Discussion	8
Summary	16
COMPARISON OF SUBSTRATES FROM TWO DIFFERENT COMMERCIAL SOURCES	31
Introduction	31
Experimental	33
Results and Discussion	34
Summary	38
EXPERIMENTAL ARTIFACTS	50
Introduction	50
Experimental	51
Results and Discussion	52
Summary	58
DESCRIPTION OF THE ULTRAHIGH VACUUM SURFACE FACILITY	67
CONCLUSION	71
REFERENCES	73
BIOGRAPHICAL SKETCH	77

Abstract of Dissertation Presented to the Graduate School
of the University of Florida in Partial Fulfillment of the
Requirements for the Degree of Doctor of Philosophy

SURFACE CHARACTERIZATION STUDY OF
InP(100) SUBSTRATES

By

Stuart Jamison Hoekje

August, 1990

Chairman: Gar B. Hoflund
Major Department: Chemical Engineering

A surface characterization study using electron spectroscopy for chemical analysis (ESCA), Auger electron spectroscopy (AES), and ion scattering spectroscopy (ISS) has been performed on InP(100) substrates. The native oxides on the surfaces were analyzed after the application of various substrate cleaning techniques including solvent cleaning, ozone etching, and two different wet chemical etching processes. The data obtained from the substrate cleaning study indicated that these surfaces are very complex and that the compositions and chemical species present vary considerably with the substrate cleaning technique used. Solvent-cleaned substrates from two different commercial sources were then examined. The data from this study show that the composition and chemical states present at the two surfaces vary considerably, which explains why substrates from different sources must be treated differently to optimize the properties of the films grown on these substrates. The third surface characterization study examined solvent-cleaned, native oxides and sputter-cleaned, InP surfaces. The

data obtained indicate that the results may be difficult to interpret due to experimental artifacts including compositional alterations by ion sputtering and electron stimulated desorption (ESD) and chemical state alteration. This combination of surface science techniques is important because ISS, AES, and ESCA probe varying depths beneath the surface. When used carefully, these techniques yield a nondestructive depth profile of the near surface region of the sample.

INTRODUCTION

Indium phosphide (InP) is a high mobility, direct band gap semiconducting material. It is a III-V compound, so named because the metal is in the group IIIA column and the non-metal is in the group VA column. A number of binary III-V compounds are presently being explored for use in electronic devices. Examples of these are gallium arsenide (GaAs), gallium phosphide (GaP) and indium antimonide (InSb). There are also ternary and quaternary III-V compounds of interest including aluminum gallium arsenide ($Al_xGa_{1-x}As$) and indium gallium arsenide phosphide ($In_xGa_{1-x}As_yP_{1-y}$). Most III-V compounds are direct band gap semiconductors, meaning that the conversion of photons to variance in electron chemical state, or vice versa, is a direct process and does not involve a third particle, such as a phonon. Charge carriers, electrons or holes, move more quickly through III-V materials than elemental semiconductors. This ease of movement, mobility, is defined as the ratio of the absolute velocity of the charge carriers to the electric field [1]. Indium antimonide has a mobility approximately 40 times larger than silicon. However the mobility of InP to silicon is only 2:1 and the primary interest in this material is due to its direct band gap, approximately 1.35 eV [2].

Direct band gap semiconducting materials are called photonic materials. Devices made from photonic materials can act as transducers, converting light into electric current as in a solar cell, or current

into light as in a solid state laser. Due to the shorter wavelength of light, approximately 5,000 A, a modulated beam can carry a greater density of information than an electrical signal. For this reason communication circuits based on photonic materials transmit information at a lower cost. The frequency of light emitted by a solid state laser is a function of its band gap. The frequency of light required varies from application to application. As such the desired band gap varies. Each compound III-V semiconductor has a different band gap. Also the ternary and quaternary compound semiconductors have band gaps that change as a function of composition [3].

The first published article on III-V electronic properties appeared in 1952 [4]. Gallium arsenide was the compound most frequently examined [5] and used for the construction of devices. A thorough review of major properties of GaAs was published in 1982 by Blakemore [6]. In 1970 InP started to attract attention from the electronic device community with the invention of the three-level, microwave oscillator [7]. At approximately the same time Blom and Woodall observed that the narrow line width of the spectra of InP solid state laser made them efficient pumps for multiphoton phosphors, furthering the application interest in InP [8]. Subsequent investigations of InP have examined optical properties [9], atomic and electronic structures [10], valence band density of states [11], and electronic surface properties [12]. Razeghi has published a recent review of InP and related compounds and growth techniques [13].

Epitaxial films of III-V materials are grown on substrates with equivalent crystalline structure and lattice constants. The two most common substrate materials are GaAs and InP. The substrates are created

by withdrawing a seed crystal from a liquid melt. This process creates a distribution of impurities throughout the crystal [14]. Phosphorus based substrates tend to degrade when heated, a necessary processing step prior to growth [15]. The substrate surface must be cleaned and polished [16]. Epitaxial growth on these substrates is accomplished by exposing the heated surface to a flux of IIIA metals and VA non-metals. This flux of materials can be supplied from a liquid source, vapor source, or molecular beam source. This distinction defines the epitaxial techniques: liquid phase epitaxy (LPE), vapor phase epitaxy (VPE) or molecular beam epitaxy (MBE). Each technique is optimal for certain applications.

Liquid phase epitaxy is inexpensive, easily controlled, well understood, and can be used on a large scale. The limitations of LPE are due to compositional and thickness variance. New devices require abrupt changes in film composition which are also beyond the capabilities of LPE. The solid state lasers used in compact disc players are aluminum gallium arsenide films grown by LPE.

There are two distinct VPE techniques, one is called the hydride process [17] and the other the metal-organic process [18]. In the hydride process film composition is thermodynamically controlled. The metal-organic process generates films whose composition is kinetically controlled. This difference allows the metal-organic process to grow a greater variety of films. There are problems with VPE. The III-V source materials are toxic, corrosive and flammable. Mathematical modeling of the growth process, in particular the fluid dynamics and kinetics, is scant. However a well designed facility can grow films with abrupt compositional changes occurring within a 10 Å region.

The MBE growth technique is capable of growing epitaxial films one atomic layer at a time [19]. This level of control allows device scientists to create layered films that exploit quantum phenomena. The large expense and limited throughput restricts MBE usage. A further difficulty with MBE is due to the high vapor pressure and reactivity of phosphorus. When phosphorus or a phosphorus bearing compound is introduced to a MBE growth chamber it adsorbs on all surfaces. All future films grown in that chamber will have traces of phosphorus. There is also difficulty in obtaining phosphorus sources of sufficient purity for quantum devices.

COMPARISON OF SUBSTRATE CLEANING TECHNIQUES

Introduction

Indium phosphide (InP) is commonly used as a substrate for epitaxially grown III-V compounds. Then these compounds are used in fabrication of electronic or opto-electronic devices due to their narrow band gaps and high electron mobilities. Binary, ternary or quaternary III-V compounds with an appropriate lattice match are grown on InP substrates by molecular beam epitaxy (MBE) [20], metalorganic chemical vapor deposition (MOCVD) [21] or chloride [22] or hydride [23] vapor phase epitaxy (VPE).

III-V compound growth on InP typically is carried out using the following procedure. An InP substrate is cleaned using one of several methods and inserted into the growth chamber. The system is purged of air and either evacuated in MBE or filled with hydrogen or helium in CVD. Then the substrate is slowly heated in an over pressure of phosphorous or a phosphorous compound in order to suppress incongruent evaporation [24]. After maintaining the sample at growth temperature (800-900K) for 10 minutes, reactants are introduced and growth on the substrate is begun [25]. It is believed that the oxide overlayer on the substrate is removed in this procedure prior to growth.

Studying the cleaning of InP substrates is important for two reasons. Firstly, InP and related materials will be used in electronic devices for many decades. Therefore, investigations which further the

understanding of the chemistry of InP and its oxides are beneficial. Secondly, it appears that certain cleaning procedures produce films of superior quality. For example, surface cleaning can induce strains which affect epitaxially grown films [26]. Since the cleaned substrate is the initial surface introduced into the growth chamber and exposed to the various pregrowth and growth conditions, it is important to characterize the species present on these substrates. As shown below, the composition and chemical nature of the InP surfaces vary significantly with the cleaning procedure used.

Native oxides of InP have been investigated by electron spectroscopy for chemical analysis (ESCA) and Auger electron spectroscopy (AES) [27], ESCA and ultraviolet photoelectron spectroscopy (UPS) [28], ESCA and secondary ion mass spectroscopy (SIMS) [29], ESCA [30] and ion scattering spectroscopy (ISS), AES and ESCA [31]. In most of these studies, the native oxide is described as a mixture of InP and oxides of In, P and InP. However, Hollinger et al. [32] considers them to be amorphous-nonstoichiometric, glass-like phases. Using techniques of varying surface sensitivity, Hoflund and Corallo [31] have shown that the native oxide which they studied has a layered nature in which different compounds lie at different depths.

Various techniques including ESCA [33], AES and photoluminescence [34,35], ellipsometry [36] and Normarski microscopy [37] have been used to examine InP substrates after wet chemical etching or sputter etching. Lau and coworkers [38-40] have used angle-resolved ESCA to determine the chemical states of In and P as a function of depth or InP substrates which were sputter etched, thermally cleaned, or ozone etched. Another ESCA investigation by Bertrand [41] examined the

chemical states of In and P remaining at the near-surface regions of InP substrates after exposure to various wet chemical etchants. Similar substrates have also been examined by Singh et al. [42] using AES.

The purpose of this present study is to characterize ozone-etched and wet-chemical-etched InP substrates using ISS, AES and ESCA. Since the surface sensitivities of these techniques vary, it is possible to obtain depth-sensitive information using this particular combination of techniques. Such a comparison of ozone etching and wet chemical etching techniques has not appeared in the literature previously.

Experimental

Sulfur-doped, N-type, InP substrates with a carrier concentration of 8×10^{18} cc^{-1} oriented 2° off (100) toward (110) were used in this investigation. The solvent cleaned sample was ultrasonically cleaned in toluene, acetone, trichloroethylene, acetone, and methanol (in that order). The wet-chemical etch #1 (511) consisted of solvent cleaning in acetone, propanol, methanol, and deionized water and then etching for 6 minutes in a 5:1:1 volume mixture of H_2SO_4:H_2O_2:H_2O, cleaning in deionized water and drying with flowing nitrogen. The wet-chemical etch #2 (N511) consisted of solvent cleaning in acetone, propanol, and methanol, etching for 1 minute in a 4:1 volume mixture of methanol:HNO_3, cleaning in methanol and deionized water and etching a second time for 3 minutes in a 5:1:1 volume mixture of H_2SO_4:H_2O_2:H_2O followed by cleaning with deionized water and methanol and drying with flowing nitrogen. The ozone-etched substrate was exposed for two minutes to ultraviolet light produced with a UV lamp placed 5 cm away from the sample surface. Air flowed continuously between the sample and the lamp.

Electron spectroscopy for chemical analysis, AES and ISS were performed using a double-pass, cylindrical mirror analyzer (CMA) (PHI Model 25-270 AR) contained in a vacuum system with a base pressure of below 1 x 10^{-10} Torr. ESCA data were taken in the retarding mode with a pass energy of 25 eV using a computer-interfaced, digital-pulse, counting circuit [43] and digital-filtering techniques [44]. Auger electron spectroscopy data was taken by operating the CMA in the non-retarding mode with a 0.5 V_{pp}, 5 kHz oscillation applied to the outer cylinder. A 10-μA primary-beam current was focused to a spot approximately 0.5 mm in diameter. Ion scattering spectroscopy was carried out in the nonretarding mode using a defocused primary beam of 1 keV ^4He ions (100 nA over an area 1 cm in diameter).

For each sample examined ESCA was performed first followed by AES and then ISS in order to minimize sample alteration by the primary beams. It has been shown that AES damages surfaces of III-V compounds resulting in altered AES peak shapes and locations [45]. ISS removes surface species by ion sputtering resulting in compositional changes of III-V surfaces. Sample damage has also been minimized in this study by exposing the sample to the beams for the minimum periods required to obtain reasonable signal-to-noise ratios. Damage induced at cleaned InP surfaces by ESCA, AES and ISS has been studied [46].

Results and Discussion

Auger spectra exhibiting the P, C, In and O peaks taken from the as-received sample after solvent cleaning, the O_3-etched sample and the 511-etched sample are shown in Figures 1, 2 and 3, respectively. The AES peaks obtained from the N511-etched sample are not shown because

they are nearly identical to those obtained from the 511-etched sample. It has been documented in numerous studies [45,47-52] that the In and P peak shapes and positions vary with chemical state. Furthermore, the composition of these oxide overlayers tend to vary significantly with depth [31]. These problems make quantification of d(NE)/dE data difficult so no attempt has been made to quantify the Auger spectra shown in Figure 1. Nevertheless, important information can be gained qualitatively from these spectra.

Based on the Auger spectra, it is apparent that the compositions of the chemically etched surfaces vary considerably from that of the solvent-cleaned surface and that the composition of the ozone-etched surface differs from the compositions of the 511- and N511-etched surfaces. The solvent-cleaned surface exhibits the largest O and C peaks. The shape of the C peak is characteristic of "graphitic" carbon. Although such contaminating carbonaceous deposits are usually referred to as graphitic in surface studies, they have not been carefully characterized, probably do not have a graphitic structure and may be adsorbed hydrocarbons. The shapes of both the In and P peaks differ considerably from those obtained from a clean InP surface [46] suggesting that at least a portion of both the P and In in the near-surface region are bonded to O. When only one state of In is present, its Auger feature exhibits a well-defined, doublet-peak structure in which the splitting between the peaks rises above the base-line level [53]. When two or more chemical states of In are present such as InP and In_2O_3, the doublet is not so well defined and the splitting is low as observed in Figure 1. This type of behavior is also characteristic of the In Auger feature in the N(E) spectrum [31]. The P Auger peak differs from that

of P in InP [46] in that the top portion of the most prominent peak does not rise significantly above the baseline. This fact suggests that some of the P is bonded to O as discussed below.

Both O and C Auger features obtained from the ozone-etched sample (Figure 2) are smaller than those obtained from the solvent-cleaned sample. The C peak shape is graphitic. Due to the fact that less O is present as In oxide, the splitting between the In peaks rises much higher than for the solvent-cleaned sample. The P feature differs from that of P in InP, but it is more well defined than the P feature in Figure 1 suggesting that less of the P in the near-surface region of the ozone-etched sample is bonded to O.

Judging from the Auger data, the cleanest and most InP-like samples are the wet-chemically etched (511 and N511) surfaces (Figure 3). These contain the least C and O. The In feature is nearly like that obtained from InP since the splitting rises nearly to the baseline. The P feature is also quite similar to that obtained from InP since the peaks rise above the baseline. The shape of the O peak is similar to that in Figure 1, but both of these are different from that obtained from the ozone-etched sample. This fact implies that at least a portion of the O at the ozone-etched surface is in a different chemical state than O at the solvent-cleaned or chemically etched (511 and N511) surfaces. This topic is discussed in more detail with regard to the ESCA data presented below.

Ion scattering spectroscopy spectra taken from all four cleaned surfaces are shown in Figures 4 and 5. Ion scattering spectroscopy is highly surface sensitive, essentially sampling only the outermost atomic layer, so the information which it yields is particularly interesting

when combined with AES and ESCA data. Peaks due to C, O, P and In, appear at E/E_o = 0.23, 0.39, 0.6 and 0.86, respectively. The relative cross sections of these elements vary significantly increasing with mass. A recent calibration study [54] performed on the same ISS system used in this InP study yielded an O/Ag ISS cross section ratio of about 0.045. The O/In ratio is expected to be only a little smaller than this since the mass of In is not much greater than that of Ag. Furthermore, the cross section of C is somewhat smaller than the cross section of O, and the cross section of P lies between those of O and In. Using this information, it is possible to extract semiquantitative compositional information from Figures 4 and 5.

The ISS spectrum taken from the solvent-etched surface is shown in Figure 4. It consists of C, O and In peaks with no P peak. This surface is almost covered with C and O in nearly equal amounts. Based on the cross section ratios discussed above, the outermost atomic layer of this surface consists of 5% In. The ISS spectrum obtained from the ozone-etched sample (Figure 4) differs considerably in that the C peak is diminished, the In peak is larger by a factor of about 5, and a barely distinguishable P peak appears. Further differences are observed in the ISS spectrum obtained from the 511-etched surface. In this case both the C and O peaks are diminished, the height of the In peak is significantly increased, and a more distinct P peak appears.

Very small differences also appear in the ISS spectra obtained from the 511-etched and N511-etched InP surfaces and shown in figure 5. It appears that the N511-etched surface contains slightly less O and more C, P, and In than the 511-etched surface. Generally, a trend is apparent from the ISS spectra. As the amounts of C and O present in the

outermost atomic layer decrease, the In concentration increases. The ISS data are consistent with the AES data even though AES probes more deeply beneath the surface.

An ESCA survey spectrum obtained from the solvent-cleaned surface is shown in Figure 6. Except for variations in the relative peak heights, this survey spectrum is similar to those obtained from the etched samples, so they are not shown. Peaks due to In, P, C and O are present, and the In 3d peaks are predominant since their sensitivity factor is much larger than those of C, O or P [55]. Compositional information has been obtained from these spectra based on peak area measurements and standard sensitivity factors and methods [55]. The compositions determined in this manner are presented in Table I for the four samples examined. These results vary considerably from the ISS and AES results since ESCA probes more deeply beneath the surface and, therefore, averages over a greater volume of the near-surface region of the solid with the more deeply lying regions contributing less to the signal. Both the compositions and the In-to-P ratios vary considerably with the cleaning method used. The solvent-cleaned sample contains the least In + P (or the most C + O), and the wet-etched surfaces contain about 40% more In + P than the solvent-cleaned or ozone-etched surfaces. The ozone-etched surface contains the greatest atomic fraction of O, which is expected. The N511-etched surface contains significantly more C than the 511-etched surface, which cannot be explained. The trend in the In-to-P ratio is interesting. It seems that more oxidizing etching treatments produce surfaces with larger In-to-P ratios. This suggests that an oxidizing environment provides a chemical driving force which enriches the near-surface region in In, since In is more readily oxidized than P.

High-resolution In, P, O and C, ESCA peaks obtained from the four cleaned or etched InP surfaces are shown in Figures 7 to 10, respectively. Significant variations in the peak shapes and positions are observed in all four sets of spectra. This indicates that the nature of the chemical species present at a cleaned or etched InP surface depend upon the surface preparation method used. Electron spectroscopy for chemical analysis has been used to examine species present at native oxide surfaces on InP in numerous studies. Many ESCA binding energy assignments have been made in these studies, and some but not all are listed in Table II. Generally, the ESCA spectra obtained from these surfaces are complex, and the instrumental resolution is not high enough to resolve peaks due to different species. These problems have introduced ambiguities into the interpretations. The ESCA binding energies used in this study are given in Table III. Spectral features appear in Figures 7 to 10 which cannot be identified using the assignments given in Table III or standard compilations [55]. Based on results obtained in another related study on experimental artifacts in surface characterization studies of InP [46], it is not believed that these features are due to charging or differential charging. It may be possible to identify these species using other surface characterization techniques, but this has not been done in this study. Instead, peaks due to their presence is noted, but accurate assignments of the species from which these peaks originate cannot be made without further effort.

The In 3d peaks shown in Figure 7 indicate that the predominant In features on all four surfaces are due to InP and In_2O_3. The nonsymmetrical shapes on the low-binding, energy side suggests that some elemental In may be present, and the shoulder on the high-binding,

energy side is due to $InPO_4$ and possibly $In(OH)_3$. This shoulder is largest for the solvent-cleaned sample, followed by that from the ozone-etched sample. An unidentified species seems to yield a shoulder on the predominant peaks at 444.2 eV. Another unidentified species appears to be present at 444.9 eV. Its presence is most apparent due to a shoulder on the spectrum obtained from the solvent-cleaned sample. The P 2p peaks shown in Figure 8 indicate that P is present as InP, elemental P and $InPO_4$. InP seems to be a predominant form of P with $InPO_4$ present in small amounts. A significant amount of elemental P is present on all four surfaces, but its presence is particularly noticeable on the ozone-etched surface. A peak from an unidentified P species lies at 127.8 eV, which is also most prominent on the spectrum from the ozone-etched surface. The P peak shapes obtained from all four samples suggest that another state of P may be present which has a P 2p binding of about 129.3 eV. The shape of the smaller peak due to $InPO_4$ at about 132 to 135 eV varies with sample treatment. It is possible that this variation is due to the presence of $(PO_3)^{-1}$, $(HPO_3)^{-2}$, $(HPO_4)^{-2}$ or $(H_2PO_4)^{-1}$ in varying amounts. It is also possible that an electron-stimulated, desorption-ion, energy distribution (ESDIED) study [56] would yield information which would allow identification of these species. A small peak at 135.0 eV in the spectrum obtained from the 511-etched sample may be due to P_2O_5. Due to the solubility of P_2O_5, it probably was removed before analysis of the samples.

The O 1s peak shapes shown in Figure 9 are quite complex and variable. This figure is particularly illustrative with regard to showing that different surface treatments alter the chemical nature of the surface. At least seven different chemical states of O are present on

these surfaces, and the relative amounts of these species vary dramatically on the four surfaces examined. Peaks due to In_2O_3, $InPO_4$ and $In(OH)_3$ are present as well as unidentified features at 529.2, 530.6, 531.2, 533.2 and 533.7 eV. Each of the unidentified features is quite prominent in at least two of the spectra. The spectrum obtained from the ozone-etched surface is quite different from the other three spectra. The predominant feature is due to an unidentified species with a binding energy of 531.2 eV, but the peak is broad due to a high-binding, energy shoulder ($InPO_4$ and/or $In(OH)_3$) and a low-binding, energy shoulder (In_2O_3). It also contains a very pronounced shoulder due to an unidentified species at 529.2 eV. It is interesting to note that this same feature is prominent in the spectrum obtained from the N511-etched surface. This is probably due to the fact that the N511 treatment is quite oxidative like the ozone treatment. The same state of O is present on the solvent-cleaned and 511-etched surfaces, but just as a small shoulder. The O 1s spectra obtained from the solvent-cleaned and 511-etched surfaces are quite similar, but the spectra obtained from the N511-etched and 511-etched surfaces are quite different. This fact demonstrates that the influence of nitric acid during the etching process is quite significant.

The C 1s peak shapes shown in Figure 10 also vary significantly, and peaks or shoulders due to at least seven different C species are apparent at 281.2, 282.7, 284.6, 285.0, 286.0, 287.8 and 289.6 eV. These facts indicate that the chemical interaction of the treated surfaces toward C-containing compounds present during the treatment steps or in the air differs depending upon the treatment. It is also possible that the C present on the as-received surfaces is modified chemically

during the various treatment procedures. Although C is nearly always present on air-exposed surfaces, very little is known about the structure or composition of these C phases. It is clear from the ESCA data presented in Table I and Figure 10 that the C is present on these surfaces in large amounts and that the chemical nature of the C-containing species is varied and complex. By examining standard compilations of binding energies of C-containing species [55], it is possible to suggest the following tentative assignments for some of the species responsible for peaks or shoulders in Figure 10: 281.1 - a carbide, 284.6 - adsorbed hydrocarbons, 286.0 - alcohol-like, organic species, 287.9 - Me_2CO and 289.6 - bicarbonate.

Summary

Electron spectroscopy for chemical analysis, AES and ISS have been used to analyze native oxide surfaces on InP(100) after solvent cleaning, ozone etching, and wet-chemical etching (511 and N511 treatments). This combination of techniques provides interesting information about these surfaces since they probe to different depths beneath the surface. They also provide different types of compositional and chemical-state information. Such a complete understanding of these surfaces would not be gained by the use of only one of these techniques.

Ion scattering spectroscopy data show that the outermost atomic layers of the four cleaned or etched InP surfaces contain primarily C, O and In and very little or no P. The solvent-cleaned surface contains the largest amounts of O and C, and the wet-chemical, etched surfaces contain the least amounts of O and C in the outermost atomic layers. The outermost layer concentration of In increases as those of O and C decrease.

Auger data show that the relative amounts of C, O, P and In in about the outermost 25 A of the solids vary considerably. The general compositional trends tend to be consistent with those of the ISS data. The solvent-cleaned sample contains the most C and O in the near-surface region followed by the ozone-etched sample and the wet-chemical etched samples. Contrasted with the ISS data, a large P peak appears in the Auger spectra, and the P-to-In ratios increase as the O and C contents decrease. Chemical state information is also gained from the Auger peak shape information. As the O contents of the near-surface regions decrease, the P and In features become more InP-like.

ESCA data provide both compositional information about the outermost 40 to 50 A region and chemical-state information. The ozone-etched surface contains the most O as expected, and the In-to-P ratio increases as the surface treatment becomes more oxidizing. The high-resolution, ESCA spectra show that a large number of chemical species of In, P, O and C are present at all four surfaces and that the types and relative amounts of surface species present vary dramatically with the cleaning or etching technique used. Further studies using other surface characterization techniques will be necessary in order to specify the chemical species present on these complex surfaces.

TABLE 1

Composition (at %) Determined from ESCA Data Obtained from Cleaned and Etched, InP Surfaces

Substrate	P	C	In	O	In + P	In:P
Solvent Cleaned	14.5%	42.9%	16.4%	26.3%	30.9%	1.13
Ozone Etch	12.7%	33.1%	19.7%	34.6%	32.4%	1.56
5:1:1 Etch	20.1%	29.6%	24.6%	25.7%	44.7%	1.22
HNO_2 5:1:1	16.5%	37.7%	22.6%	23.6%	39.1%	1.37

TABLE 2

ESCA Binding Energies Of In, P and O, Species on Native Oxides of InP from Previous Studies

Compound	P	In	O
InP	129.0 [37]	444.7 [37]	
	128.8 [26]	444.5 [26]	
	128.8 [31]	444.4 [31]	
	129.2 [57]	444.3 [57]	
		444.6 [27]	
		444.0 [51]	
In		443.6 [51]	
		443.6 [29]	
		443.8 [40]	
		444.0 [57]	
		443.6 [58]	
		443.6 [27]	
P	130.2 [27]		
	129.6 [55]		
$InPO_4$	134.1 [31]	445.7 [31]	531.8 [31]
	134.0 [57]	445.4 [57]	531.7 [57]
In_2O_3		444.7 [31]	530.2 [31]
		444.5 [58]	530.1 [58]
			530.2-530.8 [57]
		444.6 [27]	
$In(OH)_3$		445.2 [31]	531.8 [31]
P_2O_5	135.6 [31]		532.7/534.1 [31]
	136.3 [27]		
P_4O_{10}	135.5 [57]		531.7 [57]

TABLE 3

ESCA Binding Energies Used to Evaluate
Chemical States in This Investigation

Compound	P	In	O
InP	128.8	444.5	
In		443.6	
P	130.2		
$InPO_4$	134.0	445.6	531.8
In_2O_3		444.6	530.2
$In(OH)_3$		445.2	531.8

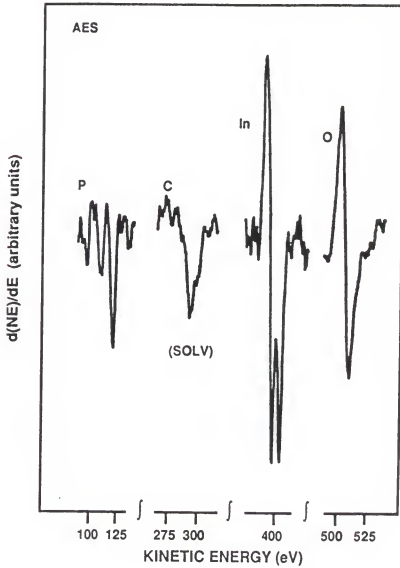

Figure 1. Auger spectrum obtained from the solvent-cleaned, InP surface.

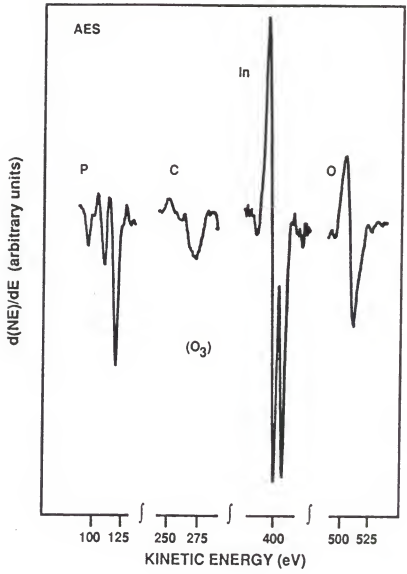

Figure 2. Auger spectrum obtained from the ozone-etched, InP surface.

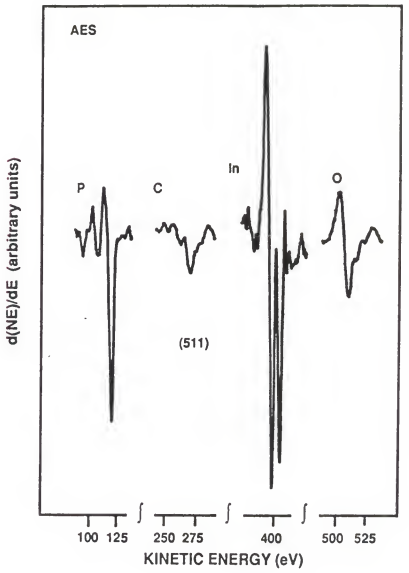

Figure 3. Auger spectrum obtained from the 511-etched, InP surface. The Auger spectrum obtained from the N511-etched, InP surface is very similar to this spectrum.

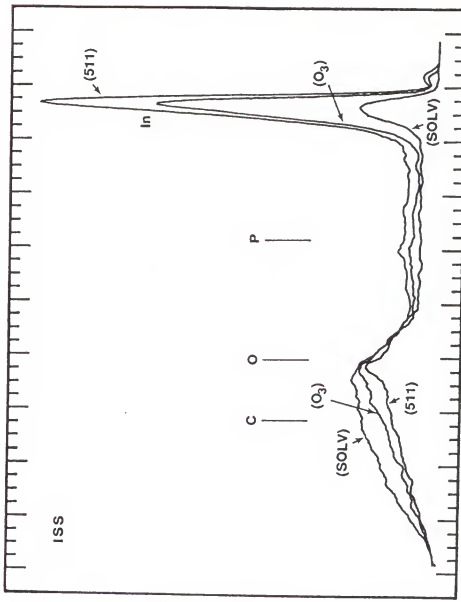

Figure 4. ISS spectrum obtained from the solvent-cleaned, ozone-etched and 511-etched, InP surfaces.

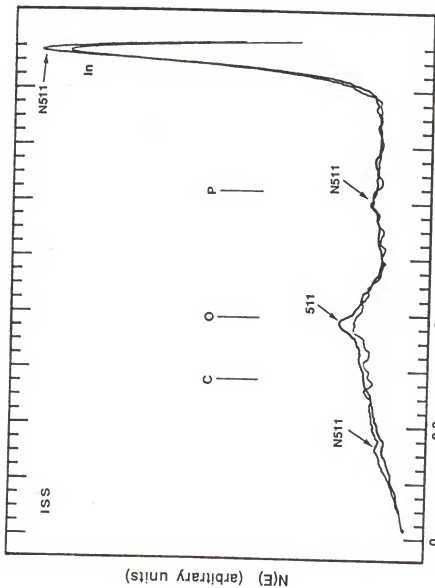

Figure 5. ISS spectra obtained from the 511-etched and N511-etched, InP surfaces.

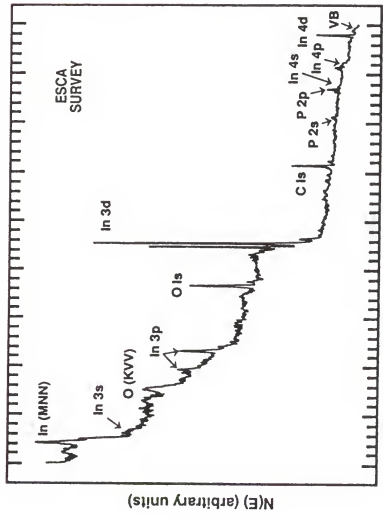

Figure 6. Survey ESCA spectrum obtained from the solvent-cleaned, InP surface. The survey spectra obtained from the ozone-etched, 5:1:1-etched and N5:1:1-etched, surfaces are similar except for variations in the relative peak heights.

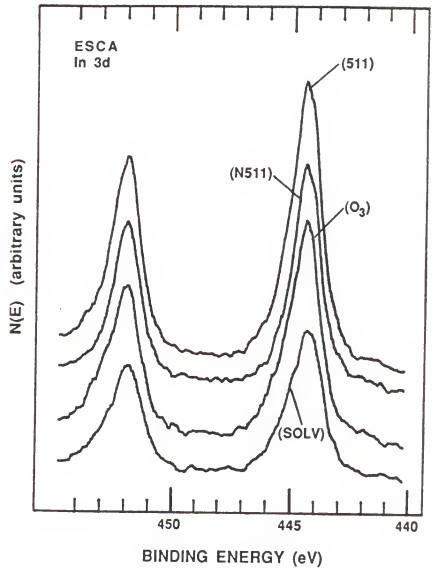

Figure 7. ESCA In 3d peaks obtained from the cleaned and etched, InP surfaces.

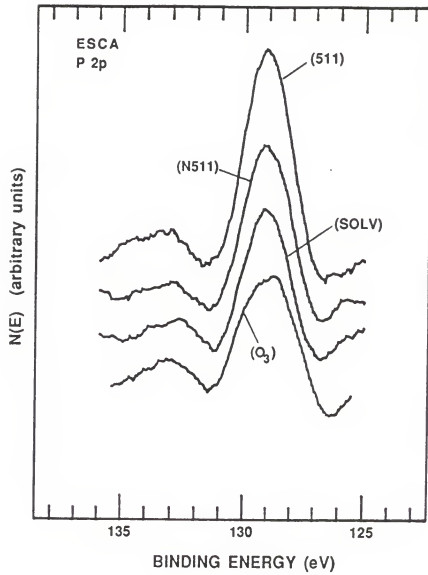

Figure 8. ESCA P 2p peaks obtained from the cleaned and etched, InP surfaces.

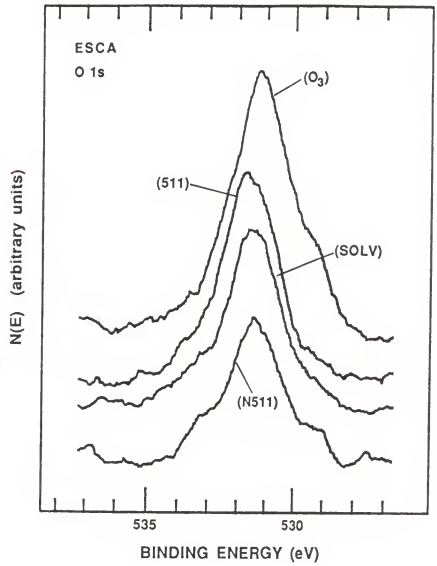

Figure 9. ESCA O 1s peaks obtained from the cleaned and etched, InP surfaces.

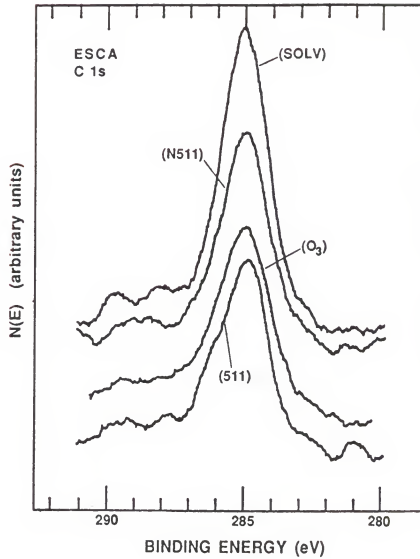

Figure 10. ESCA C 1s peaks obtained from the cleaned and etched, InP surfaces.

COMPARISON OF SUBSTRATES FROM TWO DIFFERENT COMMERCIAL SOURCES

Introduction

Indium phosphide (InP) substrates are used for the epitaxial growth of InP and other III-V compound such as $In_{(1-x)}Ga_xAs_yP_{(1-y)}$, which has the same lattice constant as InP (5.869Å) if x and y satisfy the following two constraints: $1 \geq y \geq 0$ and $x/y = 0.47$. If y=1, then the constraints indicate that the ternary compound $In_{.53}Ga_{.47}As$ has the same lattice constant as InP. These compounds are grown on InP substrates using either vapor phase epitaxy (VPE) or molecular beam epitaxy (MBE).

The surfaces of as-received InP substrates consist of a thick (>30Å) native oxide overlayer. This native oxide layer consists of a mixture of many compounds including indium oxides, phosphorus oxides, and indium phosphide oxides [31]. Hydrogen is also a component, but its presence is usually neglected since most commonly used surface characterization techniques are relatively insensitive to hydrogen. The growth of device-quality epitaxial layers requires an atomically clean and ordered substrate surface which is free of native oxide compounds and other contaminants. The removal of the native oxide prior to epitaxial growth is often done in a two-step process, one outside the growth chamber and one within the growth chamber. The initial treatment of the native oxide outside the growth chamber is accomplished by a combination of solvent cleaning, mechanical polishing, and chemical etching of the substrate. A characterization study of the native oxide

layers on InP(100) surfaces before and after the application of various chemical cleaning methods has been presented [46]. The prepared substrate is then placed inside the growth chamber and heated to approximately 500°C to sublime the residual native oxide. In order to avoid incongruent evaporation of phosphorus from the InP, an over pressure of phosphorus or a phosphorus-containing compound is maintained [24].

In order to obtain high-quality films, it is necessary to use different preparation methods for substrates obtained from different sources [59]. For example, InP substrates obtained from Sumitomo Industries Ltd. (SI) are inserted directly into the growth chamber without solvent cleaning or chemical etching steps. However, substrates obtained from CrystaCom, Inc. (CI) require solvent cleaning and chemical etching before insertion into the growth chamber. Only then are the quality of the films grown on both substrates comparable. The fact that SI substrates do not require treatment while CI substrates do suggests that the native oxides on substrates delivered from SI and CI differ. The goal of this study is to test this hypothesis. In this investigation Auger electron spectroscopy (AES), electron spectroscopy for chemical analysis (ESCA or XPS), and ion scattering spectroscopy (ISS) have been used to characterize the native oxides of InP substrates obtained from SI and CI. This particular combination of techniques is quite powerful because they probe to various depths beneath the surface. Ion scattering spectroscopy is highly surface sensitive (essentially outermost atomic layer sensitivity), and ESCA generally is the least surface sensitive. A more complete understanding of a complex surface can be gained by using all three techniques as demonstrated in a previous study [46].

Experimental

Sulfur-doped, n-type, InP substrates with a carrier concentration of 8×10^{18} cm^{-3} oriented 2° off (100) toward (110) were used in this investigation. InP substrates with identical technical specifications and physical apearance were obtained from SI and CI. Both substrates were ultrasonically solvent cleaned in toluene, acetone, TCE, acetone, and methanol (in that order).

Electron spectroscopy for chemical analysis, AES, and ISS were performed using a double-pass, cylindrical mirror analyzer (CMA) (PHI Model 25-270 AR) contained in a vacuum system with a base pressure of below 1×10^{-10} Torr. Electron spectroscopy for chemical analysis data were taken in the retarding mode with a pass energy of 25eV using a computer-interfaced, digital-pulse, counting circuit [43] and digital-filtering techniques [44]. Auger electron spectroscopy data were taken by operating the CMA in the non-retarding mode with a 0.5 V_{pp}, 5 kHz oscillation applied to the outer cylinder. A 10-μA primary-beam current was focused to a spot approximately 0.5 mm in diameter. Ion scattering spectroscopy was carried out in the non-retarding mode using a defocused primary beam of 1 keV ^4He ions (100 nA over an area 1 cm in diameter).

For each sample examined ESCA was performed first followed by AES and then ISS in order to minimize sample alteration by the primary beams. It has been shown that AES damages surfaces of III-V compounds resulting in altered peak shapes and locations [45]. Ion scattering spectroscopy removes suface species by ion sputtering causing compositional changes of III-V surfaces. Sample damage has also been minimized in this study by exposing the sample to the beams for the minimum periods required to obtain reasonable signal-to-noise ratios.

Results and Discussion

An Auger spectrum taken from the solvent-cleaned, CI-InP, substrate is shown in Figure 11. Peaks due only to P, C, In, and O are observed. This Auger spectrum is quite similar to that obtained from the SI sample so the latter is not shown. Differences include the shapes of the In and P peaks and the relative peak-to-peak heights of the In and O signals.

Determining composition from Auger peak heights is difficult due to the change in Auger peak shape with chemical state [46], the fact that the composition varies significantly with depth [31], uncertainties in mean free paths and sensitivity factors, and poorly developed models for estimating composition. Similar statements are also true for ESCA and ISS. Therefore, estimates of composition from AES, ESCA or ISS data should only be considered to be semiquantitative with only fairly large differences taken as meaningful. Compositional information obtained from Auger data using standard methods [53] are presented in Table 4. Auger analysis yields comparable concentrations of P and C for both substrates. However, the SI substrate has a 30% larger In Auger signal than the CI substrate indicating that significantly more In lies near the surface (outermost 25A) of the SI substrate. Clearly, the region sampled by AES is not stoichiometric InP since the In/P ratio is close to 2 for both samples. In fact, only about 40% of this region is In + P with the remainder being C + O. The difference in the O concentration between the two substrates is greater than those of the In, P or C. It is 40% larger for the CI substrate suggesting that the surface of the CI substrate has a more oxidic nature than the SI substrate.

The In and P Auger peak shapes also reveal important information about the chemical nature of these surfaces. Expanded In and P peaks taken from the CI and SI substrates are shown in Figures 12 and 13 respectively. With regard to the P peak, there are two important aspects of the peak shapes to consider. The first is the normalized height of the minor peak (the ratio a/c in the figures). The second is the normalized full width at half maximum (FWHM) of the major peak (the ratio b/c in the figures). When P is present only as InP, these two ratios are minimized. The ratios tend to increase as the O concentration in the near-surface region increases resulting in the presence of multiple P chemical states. The Auger In peaks behave analogously. The In peak shape characterization ratio can be defined as the normalized height of the splitting of the doublet peak structure relative to the baseline (the ratio d/e in the figures). This type of behavior is also observed for the In N(E) Auger spectrum [31].

Table 5 lists the Auger peak-shape parameters of In and P for the SI and CI, InP substrates. The P peak ratios of the two substrates differ by a factor of approximately 1.5, and the In peak ratios differ by a factor of approximately 3.5. This indicates that there is a greater mixture of chemical states for both P and In present in the near-surface region of the CI substrate than the SI substrate. Specifically, these results show that the native oxide on the CI substrate contains more In oxides and P oxides than the SI substrate in the volume probed by AES, which is consistent with the fact that the CI substrate contains about 40% more O in this region than the SI substrate (see Table 4).

Ion scattering spectroscopy spectra obtained from the CI and SI, InP substrates are shown in Figures 14 and 15, respectively. Ion scattering spectroscopy peaks due to various elements present on the SI and CI surfaces appear at the following E/E_o for the scattering angle used in this study: B-0.18, C-0.26, N-0.32, O-0.38, F-0.44, P-0.6, Cl-0.66, K-0.71 and In-0.86. The relative ISS cross sections of these elements increase quite significantly as the mass increases. A recent calibration study [54] performed in the same UHV system used in this InP study determined an ISS O/Ag cross section ratio of approximately 0.045. Since In is about 8 amu more massive than Ag, the O/In ratio would be slightly smaller. Furthermore, the cross section of C is slightly less than the cross section of O, and the P cross section lies between those of O and In.

The CI-InP substrate yields an ISS spectrum which contains peaks due to many elements including B,C,N,O,F,P,Cl and In. The predominant peaks are due to In, O and C, and very small peaks due to P and Cl are present. Based on the cross section discussion above, the outermost atomic layer of this surface contains approximately 5% In (even though the In peak is quite large) with the rest consisting mostly of C and O. The ISS spectrum obtained from the SI substrate differs markedly. It contains peaks due to C,N,O,P,K and In but none due to B or F. Again, the In peak and peaks due to the lighter contaminants are predominant, but the relative amounts are different than on the CI substrate. The outermost atomic layer of the SI substrate contains more In and less C,N and O, and the C/O ratio is smaller. The P peak is also larger and better defined. In agreement with previous studies of native oxide layers at InP surfaces [31,46], the ISS P peak is very small

compared to the In peak whether significant amounts of other contaminants are present or not.

An ESCA-survey spectrum obtained from the InP-CI substrate is shown in Figure 16. The ESCA-survey spectrum obtained from the SI substrate is nearly identical to that shown in Figure 16 so it is not shown. The ESCA-atomic, % concentrations, obtained by integrating the major-elemental, peak areas and using standard-sensitivity factors [55], for the SI and CI substrates are presented in Table 6. The composition of the regions probed by ESCA are essentially identical for the two substrates. This result is quite different than those based on the Auger and ISS data. The fact that ESCA probes more deeply than AES and ISS indicates that the compositional differences between the CI and SI substrates occur primarily in the near-surface regions of the native-oxide layers. The ESCA In/P ratio is nearly 1 for both substrates which is equal to the bulk InP ratio. Therefore, the ISS, AES and ESCA, data indicate that the In/P ratio is very high in the outermost atomic layers of these substrates and decreases to the bulk value of 1 as the depth probed increases. The difference in the C concentrations obtained from AES and ESCA data is probably due to an uncertainty in the sensitivity since the subsurface region most likely is not C rich. This assertion could be tested using angle-resolved ESCA or depth profiling, but this has not been done in this study.

Figure 17 shows a high-resolution ESCA spectrum of the P 2p region obtained from the (a) CI and (b) SI substrates. Interpretation of these spectra is based on the following binding energy assignments made in the previous study: P in InP-128.8 eV, elemental P-130.2 eV, various phosphates and biphosphates-132 to 135 eV and an unidentified P chemical

state observed in native oxides of InP at 129.3 eV [46]. Based on peak areas the surface region sampled by ESCA of the SI substrate contains four times the amounts of phosphate-like species than the CI substrate. However, the shapes of the phosphate-like peaks are different suggesting that different types of phosphate and biphosphate species are present on the two substrates. There does not appear to be any difference in the shapes of the two spectra between 127 and 131 eV except that the width is somewhat larger for the spectrum obtained from the SI substrate and the presence of the unidentified species at 127.9 eV is more pronounced on the SI substrate. These results appear to be contradictory to the results of the AES peak-shape analysis, but the differences apparently are due to the fact that ESCA probes more deeply beneath the surface than AES and the complex-layered nature of these native oxides.

Summary

A study has been carried out on the native-oxide layers of SI and CI, InP(100) substrates using ISS, AES and ESCA. This combination of techniques provides complementary information about these complex surfaces because they probe varying depths beneath the surfaces. This type of information cannot be gained through the use of only one of these techniques.

Both substrates contain large amounts of O and C, but significant differences are observed between the SI and CI substrates in the data obtained using all three characterization techniques. Ion scattering spectroscopy data show that SI substrates contain smaller amounts and fewer types of contaminating species in the outermost atomic layer than

CI substrates. Auger electron spectroscopy compositional data indicate that the region probed by AES is In depleted and O enriched on the CI substrate compared to the SI substrate. Auger electron spectroscopy In and P, peak shapes suggest that the near-surface region of the CI substrate consists of mixed chemical species to a greater extent than that of the SI substrate. Electron spectroscopy for chemical analysis probes more deeply beneath the surface than AES and ISS, and the ESCA data indicate that the elemental compositions of the two native oxides are equivalent over the region probed by ESCA. The data from all three techniques indicate that the In/P ratio is very large at the surfaces of both samples and increases to the bulk value of 1 over the volume sampled by ESCA. The differences found between the CI and SI substrates must be related to the fact that different pretreatments are required to grow high quality electronic epilayers on these two types of substrates, but the properties of the InP/native oxide interface would be most important with regard to the production of a clean and ordered InP surface used for epitaxial growth.

TABLE 4

Composition (Atomic %) Determined from AES Data Obtained from SI and CI, InP Substrates

Substrate	P	C	In	O	In + P	In/P
SI	15%	31%	31%	23%	46%	2.07
CI	13%	30%	24%	33%	37%	1.85
Sensitivity Factor (53)	0.55	0.20	0.95	0.50		

TABLE 5

Peak-Shape Parameters Determined from AES Data Obtained from SI and CI, InP Substrates

Substrate	a	b	c	d	e	a/c	b/c	d/e
SI	37	9	114	8	137	0.32	0.08	0.06
CI	39	12	88	30	132	0.44	0.14	0.23

TABLE 6

Composition (Atomic %) Determined from ESCA Data Obtained from SI and CI, InP Substrates

Substrates	P	C	In	O	In + P	In/P
SI	17%	37%	17%	29%	34%	1.00
CI	17%	40%	16%	27%	33%	0.94
Sensitivity Factor [55]	0.25	0.205	2.85	0.63		

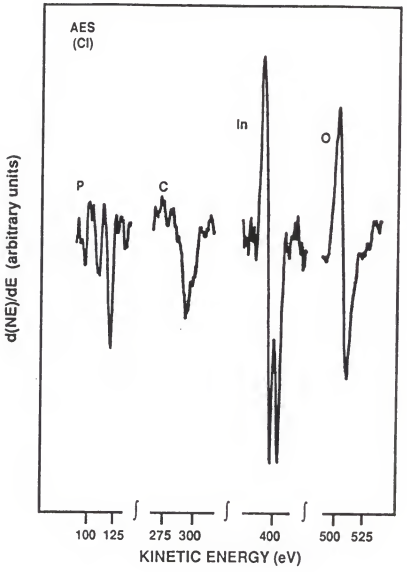

Figure 11. Auger spectrum obtained from the CI substrate.

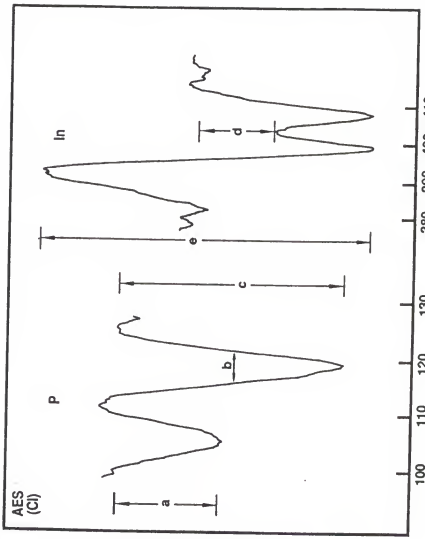

Figure 12. Expanded In and P peaks obtained from the CI substrate.

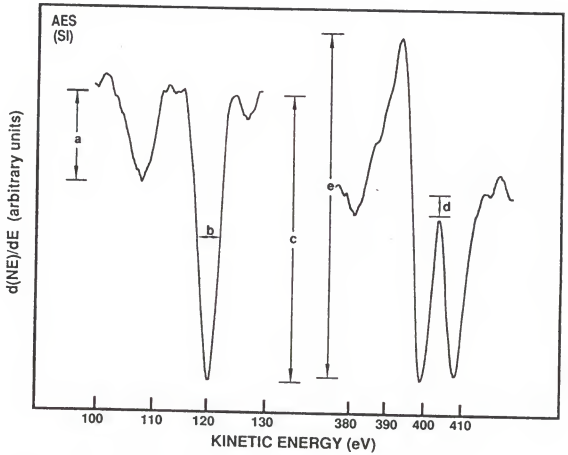

Figure 13. Expanded In and P peaks obtained from the SI substrate.

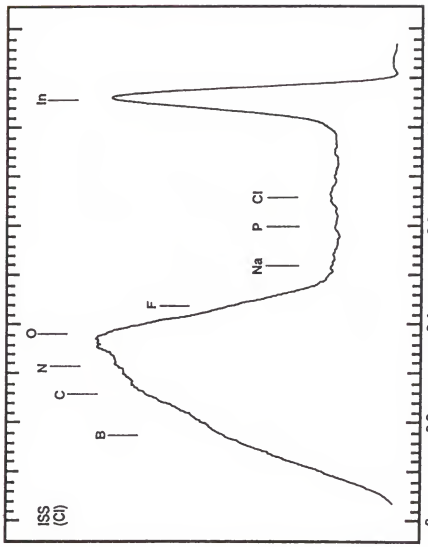

Figure 14. ISS spectrum obtained from the CI substrate.

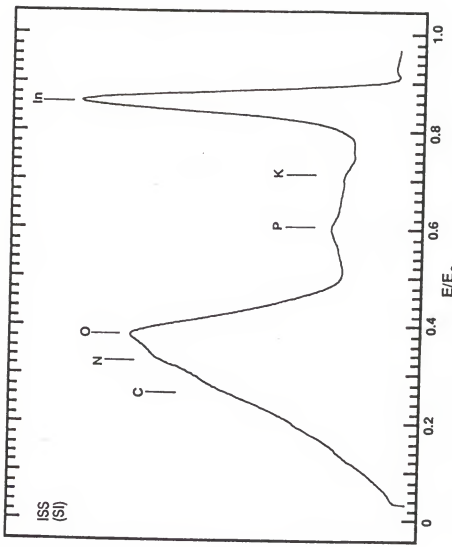

Figure 15. ISS spectrum obtained from the SI substrate.

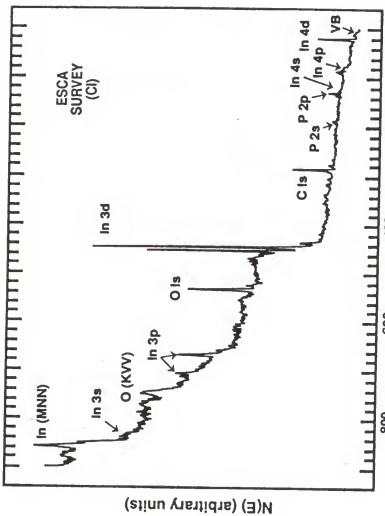

Figure 16. ESCA survey spectrum obtained from the CI substrate.

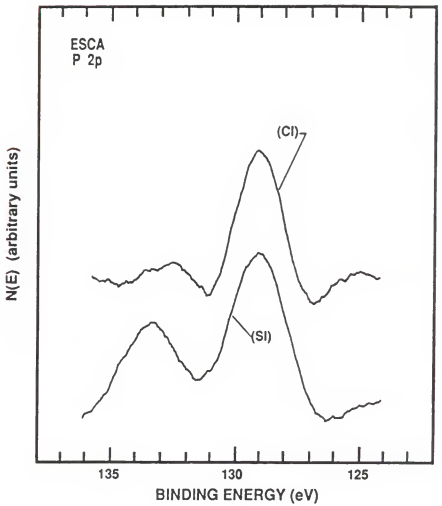

Figure 17. High-resolution ESCA P spectra obtained from the (a) CI substrate and (b) SI substrate.

EXPERIMENTAL ARTIFACTS

Introduction

Ultrahigh vacuum (UHV) surface analytical techniques have grown in popularity and use in the past 20 years. Today, it is fairly common for an analytical laboratory to have a stand-alone, computer-interfaced, Auger electron spectroscopy (AES) or electron spectroscopy for chemical analysis (ESCA) system. Other UHV surface analytical techniques including secondary ion mass spectrometry (SIMS), ultraviolet photoelectron spectroscopy (UPS), scanning Auger microscopy (SAM), scanning electron microscopy (SEM) and electron dispersive X-rays (EDX), ion scattering spectroscopy (ISS), etc. are also being used more extensively. Although the development of the field of surface science is still in its early stages, the power of these techniques has been demonstrated and is generally accepted. Unfortunately a belief has developed that the sample is inserted, an automated analysis is performed, and the concentration or other desired information is read off a computer screen or an X-Y plot. The goal of this paper is to describe some of the experimental and interpretational problems encountered in using UHV analytical techniques for analyzing surfaces of III-V compounds.

Indium phosphide is a direct band gap, high mobility III-V semiconducting material used for opto-electronic and high speed electronic devices [60]. The substrates are of interest because quality devices require epitaxially grown films of high purity, low defect concentration and precise thickness [61]. Ideally, growth of these films require a

substrate that is atomically ordered and clean. During the investigation of InP substrates using ISS, AES and ESCA, a number of experimental difficulties due to sample perturbation by the primary beams were encountered. Since these difficulties affect the analytical results and most likely apply in surface studies of other III-V materials, it is important that these experimental artifacts and their affects are recognized.

Experimental

Sulfur-doped, n-type InP substrates with a carrier concentration of 8×10^{18} cm^{-3} oriented 2° off (100) toward (110) were used in this investigation. Substrates were obtained from Sumitomo Industries, Ltd. and CrystaComm, Inc. Before analysis they were ultrasonically solvent cleaned in toluene, acetone, trichloroethylene, acetone, and methanol (in that order).

Electron spectroscopy for chemical analysis, AES and ISS were performed using a double-pass cylindrical mirror analyzer (CMA) (PHI Model 25-270 AR) contained in a vacuum system with a base pressure below 2×10^{-10} Torr. Electron spectroscopy for chemical analysis data were taken in the retarding mode with a pass energy of 25 eV using Mg Kα X-rays (PHI Model #04-151 X-ray source) and a computer-interfaced, digital-pulse, counting circuit [43] and digital filtering techniques [44]. Auger electron spectroscopy data were taken by operating the CMA in the non-retarding mode with a 0.5 V_{pp}, 5 kHz oscillation applied to the outer cylinder. A 10-μA primary-beam current was focused to a spot approximately 0.5 mm in diameter. Ion scattering spectroscopy was carried out in the non-retarding mode using a defocused primary beam of

1 keV ^{4}He ions (100 nA over an area 1 cm in diameter). For ESCA, AES and ISS, the CMA outer cylinder voltage, which is proportional to the energy of the detected particles, was generated by a model 2701C Valhalla Scientific precision DC voltage reference. This voltage was monitored by a Hewlett Packard digital voltmeter, model 3465A. The DVM measured voltage agreed with the Valhalla set voltage within 0.01 volts at all times, and the power supply was found to have less than 0.01 voltage variance for a given set point over a 24 hour period, which is near the stability limit of the voltmeter. Annealing was performed by heating the back of the stainless steel sample holder with a filament located approximately 0.5 cm from the holder. The substrate temperature was determined using an optical pyrometer (Thermalert I.R. Thermometer, model #SL300AC). Sputtering was done with 3 KeV $^{40}Ar^{+}$ ions.

Results and Discussion

Figure 18 shows three ISS spectra taken successively from a solvent-cleaned InP substrate. In ISS noble-gas ions of low molecular weight and moderate kinetic energy (0.5 to 2 keV) are scattered off a solid surface. Due to the chemical inertness of noble-gas ions, peaks in the spectra are due to ions scattered elastically off surface atoms. Therefore, the simultaneous solution of the energy balance and momentum balance generates a functional relationship between mass of the surface atom and the energy of the elastically rebounding ion at a selected scattering angle. This technique is highly surface sensitive yielding compositional information about the outermost atomic layer since ions which penetrate beneath the surface are either neutalized or scattered inelastically. Used in conjunction with other techniques of

varying depth sensitivity, such as AES and ESCA, depth profiling information may be obtained. Even though ISS provides unique and important information about a surface, it has been used in very few characterization studies of semiconductor materials [46,31].

Each spectrum in Figure 18 contains 4 peaks due to C, O, P and In, appearing at E/E_o = 0.23, 0.39, 0.60 and 0.89, respectively. The relative ISS cross sections of these elements increase significantly as mass increases. This point is demonstrated in a recent calibration study performed on the same system used in this InP study which determined an O/Ag cross section ratio of approximately 0.045 [54]. This value should only be considered as approximate since neutralization effects may vary from one type of sample to another. Considering the fact that In is about 8 amu more massive than Ag, the O/In cross section ratio would be slightly smaller than 0.045. Also, the cross section of C is slightly less than the cross section of O, and the P cross section lies between those of O and In.

Spectrum a contains a broad peak due to B, C, N and O, a very small P peak, a shoulder due to F and a large In peak. Spectra b, and c were taken after sputtering the sample for three minute intervals using the same conditions as those used to collect the ISS data. As discussed below a portion of the native oxide layer including the contaminating species are remove quite rapidly during these fairly short sputtering periods. These data demonstrate that ISS spectra should be taken with the minimum beam fluence required to give a reasonable signal-to-noise ratio and that the sample should not be exposed to ion beam except during the data collection periods.

Figure 19a and 19b are Auger spectra taken before and after the ISS shown in Figure 18 were taken. The substrate was exposed to the ion flux for approximately 3 minutes before taking the Auger spectrum in Figure 19b. The ISS results in Figure 18 demonstrate that sputtering occurs at a significant rate at these surfaces, and sputtering is known to damage III-V surfaces [62]. In agreement with the ISS data, the Auger data show a large decrease in the C signal. The AES-O, peak height does not change significantly with the sputtering treatment used. This fact appears to be at variance with the ISS results which yield a large decrease in the O signal with the sputtering treatment. The apparent discrepancy is resolved by considering the fact that AES probes much more deeply than ISS. During ISS, the outermost few atomic layers are sputtered away, and O sputters away preferentially to the In. Therefore, the sputtered-native, oxide surface then yields small C and O peaks and a large In peak in ISS. Since C is removed from the outermost few layers, it does not appear in the Auger spectra after sputtering. Although ion sputtering depletes the O in the outermost atomic layer, AES probes much more deeply and detects the subsurface O remaining in the native oxide which was not sputtered away. In fact, the fractional monolayer of O which was preferentially sputtered away is such a small amount compared to the total detected by AES that its absence does not influence the AES O-to-In peak-height ratio.

Interesting changes also occur with regard to the AES-P, peak during sputtering. Firstly, the P-to-In peak-height ratio increases with sputtering. This is primarily due to the removal of C- and O-rich layers which exposes the more P-rich, subsurface layers [46]. Secondly, very significant changes occur in the AES-P, peak shape. The P peak

obtained from the surface before sputtering is characteristic of those obtained from a mixture of phosphates, biphosphates and phosphide. The P-AES, peak shape changes considerably with chemical state. The P peak obtained from phosphates do not rise very much above the baseline whereas it does for P bonded as InP as shown in the AES spectrum of Figure 22 obtained from the sputter-cleaned, InP surface. Therefore, sputtering the native-oxide surface causes the Auger-P, peak shape to become more phosphide like as more InP is detected in the Auger signal due to removal of the outermost-surface layers. This peak-shape change introduces another problem with regard to quantification of the Auger data. It is preferable to use methods based on peak areas rather than standard methods based on peak-to-peak heights [53] for semiquantitative estimation of the near-surface composition.

Alterations of surfaces can also occur while collecting Auger spectra by electron stimulated desorption (ESD) [63]. This point is illustrated by the Auger spectra shown in Figure 20a and b which were taken before and after exposure of a solvent-cleaned, InP surface to the electron beam for 10 minutes under the same conditions used to collect Auger data. Spectrum a contains peaks due to O, In, P, C and Cl. Chlorine is a common contaminant on solvent-cleaned InP surfaces, and C usually accumulates on air-exposed surfaces due to adsorption of hydrocarbon species. During electron-beam exposure, significant changes occur. The Cl peak is reduced to about one-fourth of its original height, and the C peak height is reduced by about 20%. It appears that changes have also occurred in both the P peak shape and height, but more specific statements cannot be made in this case due to the low S/N ratio. Soonckindt et al. [45] have also observed changes in Auger peak

shapes and positions with exposure of III-V surfaces to an electron beam.

Electron spectroscopy for chemical analysis is generally considered to be less destructive than AES or ISS because the X-ray flux is low, a small fraction of the X-rays interact with the near-surface region, and the nature of the interaction usually is less destructive than sputtering or ESD. However, as shown by the following example, problems can occur in performing ESCA on semi-insulating, III-V materials which complicate data analysis and interpretation. This study was performed on the InP substrate after removal of contaminants by multiple cycles of sputter etching and annealing at 400°C. A survey ESCA spectrum, an Auger spectrum and an ISS spectrum taken from the cleaned substrate are shown in Figures 21, 22 and 23 respectively. Peaks due only to In and P appear in these spectra.

After collecting a high resolution ESCA spectrum, the first step in interpretation is adjusting the binding energy scale by a correction factor to account for the work function difference between the sample and the detector material and any charging effects. The magnitude of this correction factor is usually determined by selecting a surface species for which the binding energy is assumed to be known as the reference. Adventitious C is often used, but this may be a poor choice because its chemical state usually is not well defined or known. For the cleaned InP surface, either In or P must be chosen as the reference. The ESCA binding energy of the In $3d_{5/2}$ feature in InP is 444.5 eV [31,64,27] and 443.8 eV for In metal, and the P 2p feature in InP has a binding energy of 128.9 eV and 129.6 eV for elemental P.

Figure 23 shows the correction factor (X) required to move the In $3d_{5/2}$ binding energy to that of InP (444.5 eV) and the difference between the In $3d_{5/2}$ and P 2p binding energies (□) after the various sample treatments specified in Table 7. Generally, the difference in binding energies between the In $3d_{5/2}$ and P 2p levels (□) decreases and the correction factor increases as the X-ray exposure increases. If the X-rays do not alter the surface in some manner, then neither of these parameters would change with X-ray exposure. Furthermore, the magnitude of the change is so large that chemical state information cannot be extracted from the ESCA spectra.

Two possible explanations of the behavior shown in figure 23 are that the X-rays are inducing a change in chemical state and/or charging or differential charging are occurring. Simple charging would just shift both the In and P peaks by the same amount. One possible reaction which might be induced by X-rays is the decompositions of InP to metallic In and elemental P. If the reactions were complete in the near-surface region, then (□) would decrease by 1.4 eV which is considerably smaller than the observed decrease of 2.5 eV. However, this difference could be due to charging or differential charging of an insulating elemental P phase. The P 2p peak shape does change in progressing from a to e, and the change apparently is not reversible by sputtering or annealing treatments. These facts are consistent with the suggestion that an X-ray induced chemical reaction occurs, but further effort will be required to understand this experimental artifact.

Summary

Ion scattering spectroscopy, ESCA and AES are important techniques for the characterization of III-V semiconductor surfaces and have been used in a large number of studies. However, the application of these techniques induces changes in these surfaces, and it is important for this fact to be recognized. This study illustrates the types of changes which occur and the extent of these changes during analysis of different types of InP surfaces including the native oxide and sputter cleaned and annealed surfaces. Ion scattering spectroscopy removes the outermost surface layers by ion sputtering. Therefore, it is important to use a defocused primary ion beam and the minimum total dose to obtain a reasonable S/N ratio. Auger electron spectroscopy results in alteration of the composition of the near-surface region through the ESD process. Similar to ISS, it is preferable to use a defocused electron beam or rastor a focused electron beam and minimize beam exposure. The ESCA peak shifts and possible X-ray induced reaction was not expected and is not well understood. Further experiments need to be performed in order to understand this phenomenon which affects interpretation of the ESCA data.

TABLE 7

Sequential Treatments Performed on InP(100) Surface
Before Taking ESCA Data Shown in Figure 7

Substrate Condition	Pretreatment
a	sputter, anneal 400°C, sputter
b	anneal 400°C, 1/2 hr X-ray exposure
c	1/2 hr X-ray exposure
d	8 hr exposure, sputter 2-1/2 hrs, anneal 8 hrs
e	1/2 hr X-ray exposure

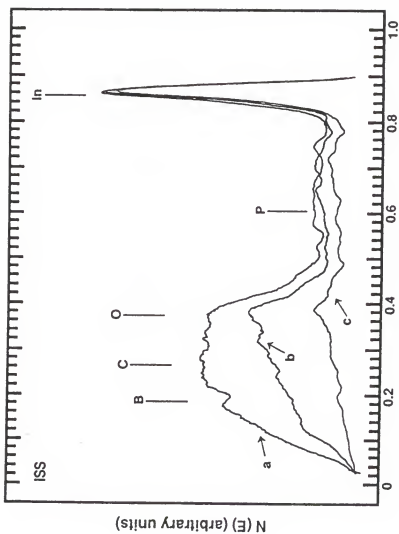

Figure 17. ISS spectra taken from the native oxide on InP(100) after 3 minute sputtering periods using the same sputtering conditions as those used to take the ISS data.

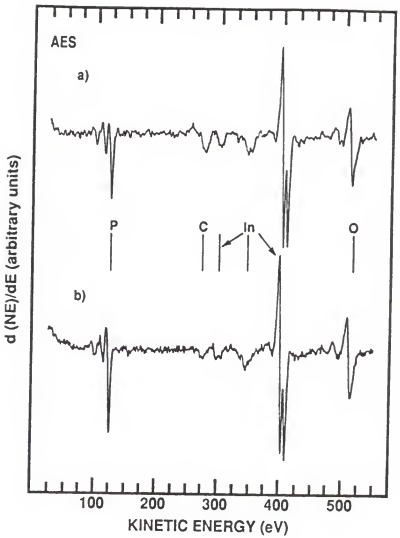

Figure 18. Auger spectra taken from the native oxide on InP(100) (a) before and (b) after ion sputtering for 3 minutes using $^{4}He^{+}$ and the same conditions used to collect ISS data.

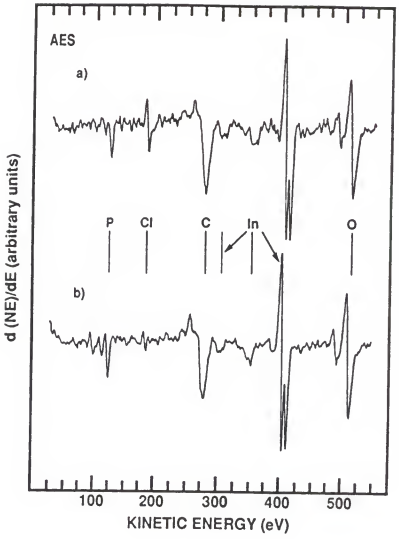

Figure 19. Auger spectra taken from a chemically etched InP surface (a) before and (b) after exposure to the electron beam for 10 minutes under the same conditions used to collect Auger spectra.

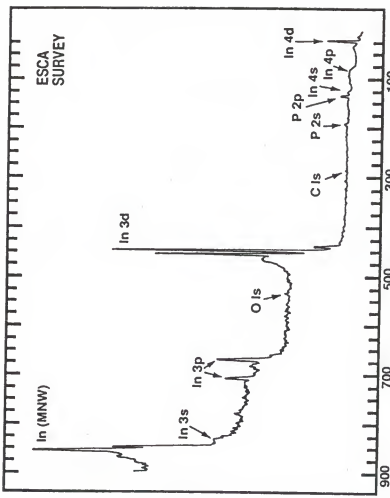

Figure 20. Survey-ESCA spectrum taken from the sputter-cleaned and annealed, InP(100) surface.

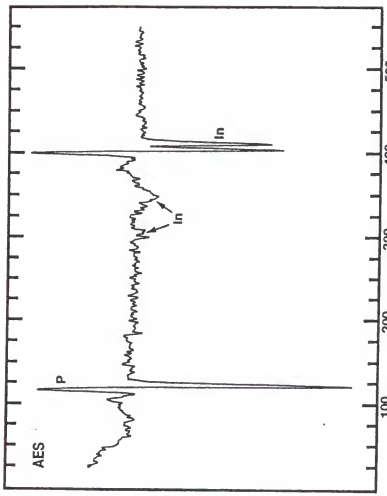

Figure 21. Auger spectrum taken from the sputter-cleaned and annealed, InP(100) surface.

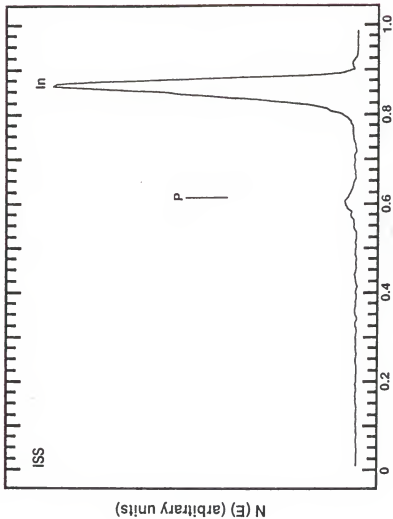

Figure 22. ISS spectrum taken from the sputter-cleaned and annealed, InP(100) surface.

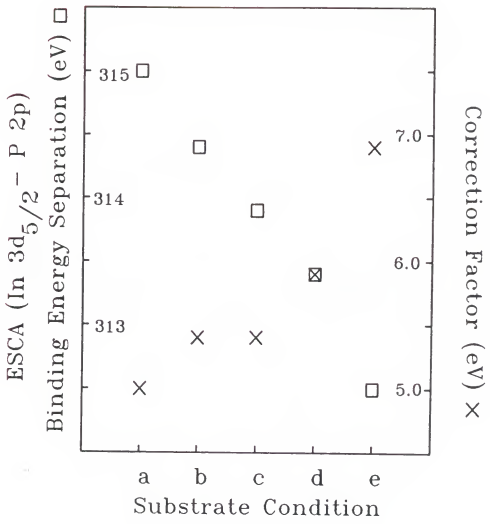

Figure 23. ESCA (In $3d_{5/2}$ - P 2p) binding energy difference (□) and correction factor (X) obtained after various sequential sample treatments: (a) sputtered, annealed at 400°C and sputtered again, (b) annealed and exposed to X-rays for 1/2 hour, (c) exposed to X-rays for another 1/2 hour, (d) exposed to X-rays for 8 hrs and (e) exposed to X-ray for another 1/2 hr.

DESCRIPTION OF THE ULTRAHIGH VACUUM SURFACE FACILITY

A top view of the system is shown in Figure 24. This system has many unique capabilities for the study of surfaces. A system has been developed which consists of a sample preparation chamber, a pretreatment chamber, and the UHV analysis chamber. A sample manipulator system has been developed which makes it possible to move the sample betwen the various chambers and heat the sample in the preparation or analysis chamber. It is also possible to prepare model catalysts in a highly controlled atmosphere with intermediate surface characterizations. Then, the sample can be moved from the vacuum system and inserted into a high pressure reactor and back into the UHV system for analysis without exposure to air.

It is possible to prepare numerous types of catalytic surfaces in this type of system. Many of our studies have involved electrochemically prepared catalysts such as tin oxide- or titania-supported platinum. With this system oxide surfaces can be prepared and characterized in the UHV system. Facilities for metallization are also contained in the preparation chamber so that mixed oxide catalysts and supported metal catalysts can be prepared totally within the system. Furthermore, the same facilities which are used for catalyst preparation can be used for treatment of materials with high pressures of gases at temperatures up to ≈800°C.

The system utilizes ion pumping and Ti sublimation pumping to reach a base pressure in the 10^{-11} Torr range. A turbomolecular pump is used to rough the system, pump inert gas away after sputtering or performing ion scattering spectroscopy (ISS), and differentially pump other portion of the system. A PHI Model 25-270AR double-pass CMA charged-particle energy analyzer is suspended vertically from port 6. Port 5 contains a manipulator with capabilities for moving, heating, and cooling the sample. The sample is placed on this manipulator by a long stroke manipulator after sample preparation and pretreatment.

Many surface techniques are included in this UHV system (see Table 8). The CMA is used both as a charged particle energy analyzer and as a time-of-flight mass spectrometer. Numerous sources are mounted in the ports focusing at the CMA focal point including an ion gun, an ultraviolet photon generator, an X-ray source, electron guns and a molecular beam doser. This allows us to perform many techniques using the CMA including X-ray photoelectron spectroscopy (XPS), Auger electron spectroscopy (AES) and scanning Auger microscopy (SAM), electron energy loss spectroscopy (ELS), Auger electron appearance potential spectroscopy (AEAPS), electron stimulated desorption with angular resolution and energy analysis (ESD, ESDIAD, ESDIED), ultraviolet photoemission spectroscopy (UPS), ion scattering spectroscopy (ISS), and secondary ion mass spectrometry (SIMS). This chamber also contains a mass spectrometer and a secondary electron detector so that we can perform temperature programmed desorption (TPD), isotope exchange experiments, and work function measurements. It is possible to perform many of these techniques in an angularly resolved manner over a very broad temperature range from that of liquid nitrogen to above 1200°C.

TABLE 8

Available Techniques

I. Cylindrical Mirror Analyzer

- *A. X-ray Photoelectron Spectroscopy
- *B. Ultraviolet Photoemission Spectroscopy (UPS)
- *C. Auger Electron Spectroscopy (AES)
- D. Scanning Auger Microscopy (SAM)
- *E. Electron Energy Loss Spectroscopy (ELS)
- F. Auger Electron Appearance Potential Spectroscopy (AEAPS)
- *G. Electron Stimulated Desorption (ESD, ESDIED, ESDIAD)
- H. Ion Scattering Spectroscopy (ISS)
- I. Depth Profiling

II. Others

- A. Work Function Measurements
- B. Temperature Programmed Desorption
- C. Isotope Exchange Experiments
- D. Secondary Ion Mass Spectrometry (SIMS and Tandem SIMS)
- E. Gas Dosing
- F. Heating > 1500°C
- G. Cooling to 10 K
- H. Inverse Photoelectron Spectroscopy
- I. Metal Deposition
- J. High Pressure Pretreatment

*Can be performed in the angle-resolved mode

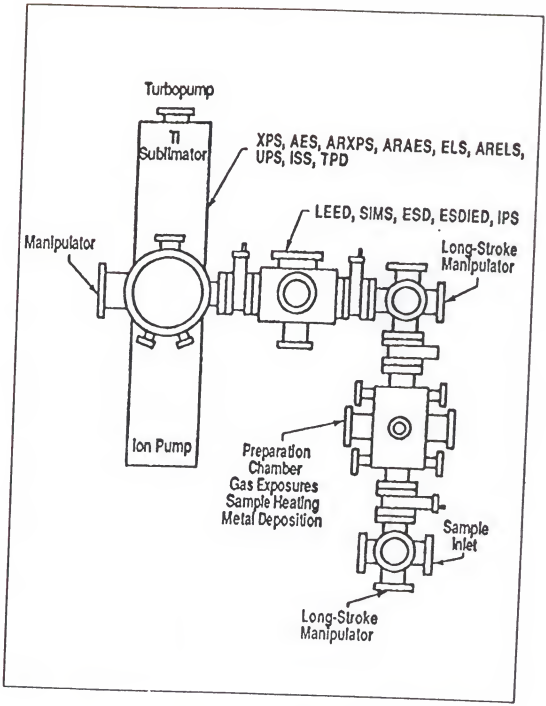

Figure 24. Schematic of ultrahigh vacuum analytical system used for study.

CONCLUSION

The combination of the surface analytical techniques of ISS, AES, and ESCA provide a nondestructive exploration of InP substrates. Sample perturbation due to these techniques has been described and optimal experimental techniques have been developed. Semiconducting materials besides InP may also be examined with this combination of techniques. These materials may be III-V, II-V, or elemental.

The examination of InP substrate preparation was an attempt to understand the differences due to each etchant. No effort was made to correlate device performance with substrate preparation. Further studies would include analyzing grown epi-layers with surface analytical techniques. Ultimately device performance as a function of substrate preparation would be explored.

Similarly the examination of substrates from different manufactures did not attempt to explain the source but to document the existence of differences in the native oxide's of InP from CrystaComm and Sumitomo. Further work would consist of interacting with the manufactures and analyzing the substrate at various stages of the manufacturing process.

The influence of x-rays on InP substrates warrants further investigation. The study should be repeated and other direct and indirect bandgap semiconductors should be examined. The work should also be repeated on stoichiometric InP.

It should be noted that all high resolution ESCA binding energies were repeatable to within 0.1 eV. The only exception was the last study where x-rays interacted with the sputter etched InP substrate and shifted the P 2p binding energy. The AES and ISS spectra used for this work was representative of numerous examinations. All qualitative trends were repeatable.

REFERENCES

1. C. Kittel in Introduction to Solid State Physics, 6th Ed., p. 204, John Wiley and Sons, New York, NY, 1986.

2. C.J. Nuese in Crystal Growth, a Tutorial Approach, p. 355, Eds. W. Bardsley, D.T.J. Hurle, and J.B. Mullin, North-Holland, Amsterdam, Holland, 1979.

3. J.M. Rowell, Sci. American 10(1986)147.

4. C. Hilsum in Progress in Semiconductors, Vol. 9, p. 135, Eds. A.F. Gibson and R.E. Burgess, Heywood, London, England, 1965.

5. H. Welker, Z. Naturforsch A 7(1952)744.

6. J.S. Blakemore, J. Appl. Phys. 53(1982)R123.

7. C. Hilsum and H.D. Rees, Electron. Letters 6(1970)277.

8. G.M. Blom and J.M. Woodall, Appl. Phys. Letters 17(1970)373.

9. E.W. Williams, W. Elder, M.G. Astles, M. Webb, J.B. Mullin, B. Straughan, and P.J. Tufton, J. Electrochem. Soc. 120(1973)1741.

10. X. Wang, Appl. Sur. Sci. 33/34(1988)88.

11. C.J. Vesely and D.L. Kingston, Phys. Rev. B 8(1973)2685.

12. J. van Laar, A. Huijser, and T.L. van Rooy, J. Vac. Sci. Technol. 14(1977)894.

13. M. Razeghi in The MOCVD Challenge, Vol. 1, p. 29, Ed. C. Hilsum. Adam Hilger, Bristol, England, 1989.

14. Y. Hayakawa, Y. Saitou, Y. Sugimoto, and M. Kumagawa, J. Elect. Mat. 19(1990)145.

15. F. Genova, C. Papuzza, C. Rigo, and S. Stano, J. Cryst. Growth 69(1984)635.

16. R.P. Vasquez, B.F. Lewis, and F.J. Grunthaner, J. Vac. Sci. Technol. B 1(1983)791.

17. M.J. McCollum, M.H. Kim, S..S. Bose, B. Lee, and G.E. Stillman, Appl. Phys. Letts. 53(1988)1868.

18. A.W. Nelson, P.C. Spurdens, S. Cole, R.H. Waling, R.H. Moss, S. Wong, M.J. Harding, D.M. Cooper, W.J. Devlin, and M.J. Robertson, J. Cryst. Growth 93(1988)792.

19. C.E.C. Wood in Physics of Thin Films, Vol. 11, p. 35, Eds., G. Haas and M.H. Grancombe, Academic Press, New York, NY, 1980.

20. A.Y. Cho, Thin Solid Films 100(1983)291.

21. H.M. Manasevit and W.S. Simpson, J. Electrochem. Soc. 116(1969)1725.

22. J. Chevrier, E. Horache and L. Goldstein, J. Appl. Phys. 53(1982)3247.

23. S.B. Hyder, J. Cryst. Growth 54(1981)109.

24. R.F.C. Farrow, J. Phys. D. (Appl. Phys.) 7(1974)2436.

25. A. Howard, personal communication.

26. Z. Hang, H. Shen and F.H. Pollak, J. Appl. Phys. 64(1988)3233.

27. J.H. Thomas III, G. Kaganowicz and J.W. Robinson, J. Electrochem. Soc. 135(1988)1201.

28. J.F. Wager, D.L. Ellsworth, S.M. Goodnick and C.W. Wilmsen, J. Vac. Sci. Technol. 19(1981)513.

29. A. Nelson, K. Geib and C.W. Wilmsen, J. Appl. Phys. 54(1983)4134.

30. D.T. Clark, T. Fox, G.G. Roberts and R.W. Sykes, Thin Solid Films 70(1980)261.

31. G.B. Hoflund and C.F. Corallo, Surf. Interface Anal. 9(1986)319.

32. G. Hollinger, E. Bergignat, J. Joseph and Y. Robach, J. Vac. Sci. Technol. A 3(1985)2082.

33. R.P. Vasquez, B.F. Lewis and F.J. Grunthaner, J. Vac. Sci. Technol. B 1(1983)791.

34. S.K. Krawczyk, M. Garrigues and H. Bouredoucen, J. Appl. Phys. 60(1986)392.

35. R.R. Chang, R. Iyer and D.L. Lile, J. Appl. Phys. 61(1987)1995.

36. D. Gautard, J.L. Laporte, M. Cadoret and C. Pariset, J. Cryst. Growth 71(1985)125.

37. A. Saletes, F. Turco, J. Massies and J.P. Contour, J. Electrochem. Soc. 135(1988)504.

38. W.M. Lau, R.N.S. Sodhi, B.J. Flinn, K.H. Tan and G.M. Bancroft, Appl. Phys. Lett. 51(1987)177.

39. W.M. Lau, R.N.S. Sodhi and S. Ingrey, Appl. Phys. Lett. 52(1988)386.

40. S. Ingrey, W.M. Lau, N.S. McIntyre and R. Sodhi, J. Vac. Sci. Technol. A 5(1987)1621.

41. P.A. Bertrand, J. Vac. Sci. Technol. 18(1981)28.

42. S. Singh, R.S. Williams, L.G. Van Uitert, A. Schlierr, I. Camlibel and W.A. Bonner, J. Electrochem. Soc. 129(1982)447.

43. R.E. Gilbert, D.F. Cox and G.B. Hoflund, Rev. Sci. Instrum. 53(1982)1281.

44. J. Olivier, P. Faulconnier and R. Poirier, J. Appl. Phys. 51(1980)4990.

45. L. Soonckindt, J. Bonnet, H. Mansour and L. Lassabatere, Surface Sci. 162(1985)186.

46. S.J. Hoekje and G.B. Hoflund, to be published.

47. H.J. Kang, Y.M. Moon, T.W. Kang, J.Y. Leen, J.J. Lee and D.S. Ma, J. Vac. Sci. Technol. A 7(1989)3251.

48. C.W. Tu and A.R. Schlier, Appl. Surface Sci. 11/12(1982)355.

49. A. Savitzky and M.J.E. Golay, Anal. Chem. 36(1984)1627.

50. J. Massies and F. Lemaire-Dezaly, J. Appl. Phys. 55(1984)3136.

52. L.L. Kazmerski, P.J. Ireland, P. Sheldon, T.L. Chu, S.S. Chu and C.L. Lin, J. Vac. Sci. Technol. 17(1980)1061.

52. B. Achard, B. Gruzza and C. Pariset, Surface Sci. 160(1985)L519.

53. L.E. Davis, N.C. MacDonald, P.W. Palmberg, G.E. Riach and R.E. Weber, Handbook of Auger Electron Spectroscopy, Physical Electronics Industries, Inc., Eden Prairie, Minnesota (1976).

54. M.R Davidson, G.B. Hoflund and R.A. Outlaw, to be published.

55. C.D. Wagner, W.M. Riggs, L.E. Davis, J.F. Moulder and G.E. Muilenberg (ed.), Handbook of X-ray Photoelectron Spectroscopy, Perkin-Elmer Corporation, Eden Prairie, Minnesota (1979).

56. G.B. Hoflund, Scanning Electron Microscopy IV(1985)1391.

57. M. Fathipour, P.K. Boyer, G.J. Collins and C.W. Wilmsen, J. Appl. Phys. 57(1985)637.

58. A.W.C. Lin, N.R. Armstrong and T. Kuwana, Anal. Chem. 49(1977)1228.

59. C. Park, personal communications.

60. E.W. Williams, W. Elder, M.G. Astles, M. Webb, J.B. Mullin, B. Straughan and P.J. Tufton, J. Electrochem. Soc. 120(1973)1741.

61. A.W. Nelson, P.C. Spurdens, S. Cole, R.H. Walling, R.H. Moss, S. Wong, M.J. Harding, D.M. Copoper, W.J. Devlin and M.J. Robertson, J. Cryst. Growth 93(1988)792.

62. Osamu Wada, J. Phys. D: Appl. Phys. 17(1984)2429.

63. G.B. Hoflund, Scanning Electron Microscopy IV(1985)1391.

64. Z. Hang, H. Shen and F.H. Pollack, J. Appl. Phys. 64(1988)3233.

BIOGRAPHICAL SKETCH

The author was born on July 30, 1955, in Washington, D.C., to James Wilbur and Cleora Ann Hoekje. The author was raised in Illinois in the northwest suburbs of Chicago, where he attended high school in Wauconda, Illinois. He graduated in 1973 and attended Western Illinois University in Macomb between 1973 and 1975, majoring in physics. The author transferred to the University of Illinois, Urbana, and received a B.S. in Chemical Engineering in 1978. He was employed by IBM in San Jose, California, until 1981, working as a development engineer on thin film memory heads. In 1982 and 1983, the author traveled throughout California, Washington, Arizona and Oregon and pursued personal interests. In 1984 the author moved to northern Michigan and lived in a small cabin, near Good Hart, cutting wood and carrying water. In 1985 the author was employed by Professor Richard C. Alkire, department chairman of the Chemical Engineering Department of the University of Illinois, as a plasma research engineer. At Dr. Alkire's suggestion the author attended the University of Florida and received his M.S. in chemical engineering in 1986. The author plans to receive his Ph.D. in August, 1990.

I certify that I have read this study and that in my opinion it conforms to acceptable standards of scholarly presentation and is fully adequate, in scope and quality, as a dissertation for the degree of Doctor of Philosophy.

Gar B. Hoflund, Chairman
Professor of Chemical Engineering

I certify that I have read this study and that in my opinion it conforms to acceptable standards of scholarly presentation and is fully adequate, in scope and quality, as a dissertation for the degree of Doctor of Philosophy.

Mark E. Grazem
Associate Professor of Chemical Engineering

I certify that I have read this study and that in my opinion it conforms to acceptable standards of scholarly presentation and is fully adequate, in scope and quality, as a dissertation for the degree of Doctor of Philosophy.

Dinesh O. Shah
Professor of Chemical Engineering

I certify that I have read this study and that in my opinion it conforms to acceptable standards of scholarly presentation and is fully adequate, in scope and quality, as a dissertation for the degree of Doctor of Philosophy.

Herbert A. Laitinen
Graduate Research Professor of Chemistry

I certify that I have read this study and that in my opinion it conforms to acceptable standards of scholarly presentation and is fully adequate, in scope and quality, as a dissertation for the degree of Doctor of Philosophy.

Vaneica Y. Young
Associate Professor of Chemistry

This dissertation was submitted to the Graduate Faculty of the College of Engineering and to the Graduate School and was accepted as partial fulfillment of the requirements for the degree of Doctor of Philosophy.

August 1990

for Hubert A. Bevis
Winfred M. Phillips
Dean, College of Engineering

Madelyn M. Lockhart
Dean, Graduate School